

# Approximation of Protein Structure for Fast Similarity Measures

Fabian Schwarzer  
Computer Science Dept.  
Stanford University  
Stanford, CA 94305, USA  
schwarzf@stanford.edu

Itay Lotan  
Computer Science Dept.  
Stanford University  
Stanford, CA 94305, USA  
itayl@stanford.edu

## ABSTRACT

It is shown that structural similarity between proteins can be decided well with much less information than what is used in common similarity measures. The full  $C_\alpha$  representation contains redundant information because of the inherent chain topology of proteins and a limit on their compactness due to excluded volume. A wavelet analysis on random chains and proteins justifies approximating subchains by their centers of mass. For not too compact chain-like structures in general, and proteins in particular, similarity measures that use this approximation are highly correlated to the exact similarity measures and are therefore useful, e.g., as fast filters. Experimental results with such simplified similarity measures in two applications, nearest neighbor search and automatic structural classification show a significant speed up.

## Categories and Subject Descriptors

J.3 [Life and Medical Sciences]: Biology and Genetics

## General Terms

Algorithms, Experimentation

## Keywords

protein structure, similarity measures, approximation of structure, nearest-neighbor search

## 1. INTRODUCTION

Automatic protein structure comparison is an important problem in computational structural biology, e.g., in structural databases and classification [12, 26], structure prediction [8, 9, 21, 28, 32, 33], analysis of trajectories through conformational space generated by molecular dynamics and Monte Carlo simulations [24, 31, 38], graph-based methods for evaluating ensemble properties [2, 3, 35], etc.

Permission to make digital or hard copies of all or part of this work for personal or classroom use is granted without fee provided that copies are not made or distributed for profit or commercial advantage and that copies bear this notice and the full citation on the first page. To copy otherwise, to republish, to post on servers or to redistribute to lists, requires prior specific permission and/or a fee.

RECOMB'03, April 10–13, 2003, Berlin, Germany.

Copyright 2003 ACM 1-58113-635-8/03/0004 ...\$5.00.

In contrast to sequence matching, structural matching requires a similarity measure that is based on spatial atom coordinates. Nevertheless, it is still important whether the structures that are compared have the same amino acid sequence or not. For conformational samples from the same sequence there are no ambiguities about correspondences. In this case, similarity measures such as *cRMS* or *dRMS* are commonly used [20]. These measures are defined as the root mean square (RMS) of either distances between corresponding atoms in the two compared structures (*cRMS*) or their corresponding intra-molecular distance matrix entries (*dRMS*). Comparing protein structures that derive from different sequences is more difficult because it is generally not obvious which features (atoms) of one structure should be matched with which features from the other structure. Numerous methods for finding a set of correspondences have been proposed [10, 11, 13, 15, 20, 23, 30, 34, 37]. For example, a dynamic programming approach from sequence alignment was used in [11].

Most similarity measures are based on rather fine granular feature selection. Typically, the coordinates of all  $C_\alpha$  atom centers are considered, and sometimes even those of additional atoms. For larger proteins, the number of considered features greatly affect the efficiency of the structural comparison. For example, intra-molecular distance matrices grow quadratically with the number of residues. The complexity of the dynamic programming algorithm in [11] is quadratic in the number of features. While this is not a real problem when comparing a single pair of structures (most proteins have less than 1000 residues), it becomes an important issue when querying a database for similar structures, or when clustering a large set of structures.

In this paper, we show that the complexity of similarity measures can be reduced while introducing only a small error. We uniformly sub-divide the backbone into a small number of contiguous subchains and represent each of the subchains by the average coordinates of its atom centers. Similarity measures can then be defined on these “averaged conformations”. Although this simplification introduces some error, we provide theoretical and experimental evidence that enough information about relative similarity is retained to discriminate structures in practical applications. In particular, the derived similarity measures using the averaged protein representation are highly correlated to their original full-atomic counterparts. If high accuracy is a concern, approximate similarity measures are still useful as a fast filter to considerably reduce the number of pairs that

need to be passed to the exact similarity measure. While we cannot give bounds on the error that is introduced, we show through wavelet analysis of protein structures and random chains that averaging is a reasonable method for reducing the dimensionality of structure descriptors.

Reducing the computational complexity of similarity measures significantly accelerates many tasks that involve structural matching. In our experiments we observed decreases in running times by large factors, typically from days to hours or even minutes. For very large sets of proteins, both the efficiency of structure comparison of a single pair and the number of such pairs that are actually evaluated are important. Many approaches require evaluation of all pairs (“brute-force approach”) even if the task is to identify only a small constant number of nearest neighbors for each conformation in the set. Using our averaged representation we show that we can avoid this quadratic cost of examining all pairs in a  $k$  nearest-neighbor application. In another application to automatic structural classification, the complexity of a previous algorithm that matches pairs of structures grows quadratically with the number of residues. In this case as well, a small reduction in the number of features results in substantial savings.

In Section 2, we describe in detail the proposed averaging that takes advantage of the chain and excluded volume properties of proteins. In Section 3, we demonstrate our approach in a  $k$  nearest-neighbor application on a large set of different conformations of the same sequence. In Section 4, we use our approach as a fast pre-filter to significantly speed up the STRUCTAL algorithm [11] for classification of structures with different sequences.

## 2. SHAPE SIMILARITY AND APPROXIMATION OF CHAINS

Given two sequences of points in 3-space  $P = (\mathbf{p}_1, \dots, \mathbf{p}_n)$  and  $Q = (\mathbf{q}_1, \dots, \mathbf{q}_n)$ , their coordinate root mean square deviation ( $cRMS$ ) is a common measure of similarity. It is defined as

$$cRMS(P, Q) = \min_T \sqrt{\frac{1}{n} \sum_{i=1}^n \|\mathbf{p}_i - T\mathbf{q}_i\|^2} \quad (1)$$

where  $\|\cdot\|$  is the Euclidean  $L_2$ -norm and  $T$  is a rigid body transform (rotation and translation). A closed form solution for  $T$  yields the optimal alignment [16].

Another common RMS shape similarity measure,  $dRMS$ , is based on comparing intra-set point distance matrices, i.e. the matrix of distances between all points within each structure. For a point set  $P$ , this matrix is defined as

$$(d_{ij}^P) = \|\mathbf{p}_i - \mathbf{p}_j\|. \quad (2)$$

The distance matrix RMS deviation ( $dRMS$ ) of  $P$  and  $Q$  is then defined as

$$dRMS(P, Q) = \sqrt{\frac{2}{n(n-1)} \sum_{i=2}^n \sum_{j=1}^{i-1} (d_{ij}^P - d_{ij}^Q)^2}. \quad (3)$$

When applying these similarity measures to proteins, it is common practice to use the  $C_\alpha$  atom centers, ordered along

the backbone, as defining points. (Sometimes, additional atoms are included or  $C_\beta$  atoms are used instead.) The positions of these atoms are usually considered to determine the shape of the backbone sufficiently well. However, in the case of  $dRMS$ , the intra-molecular distance matrices grow quadratically with the length of the protein, which significantly slows down the  $dRMS$  computation for large proteins.

### 2.1 Approximate similarity measures

We reduce the number  $n$  of sample points in  $P$  and  $Q$  as follows. In each sequence, we replace contiguous subsequences of points by their centroids. That is, we uniformly partition the sequence  $P$  of length  $n$  into  $m$  contiguous subsequences of length  $\lfloor n/m \rfloor$  each. (If  $n/m$  is not an integer, some subsequences will be chosen to be longer by one.) For each subsequence, we then replace its points by their centroid, which we denote by  $\bar{\mathbf{p}}_j$  for subsequence  $j$ . For example, if subsequence  $j$  spans points  $(\mathbf{p}_r, \dots, \mathbf{p}_s)$  then

$$\bar{\mathbf{p}}_j = \frac{1}{s-r+1} \sum_{i=r}^s \mathbf{p}_i. \quad (4)$$

Based on these averaged subsequences we define the  $m$ -averaged representation  $\bar{P}_m$  of  $P$  as the sequence of  $m$  points  $(\bar{\mathbf{p}}_1, \dots, \bar{\mathbf{p}}_m)$ . (For  $Q$ , we proceed in the same way.) We can now define the simplified RMS measures for  $\bar{P}_m$  and  $\bar{Q}_m$  analogously to the above RMS measures on the original sequences. That is, in the defining formulas (Equations 1, 2 and 3), we replace  $\mathbf{p}_i$  ( $\mathbf{q}_i$ ) by  $\bar{\mathbf{p}}_i$  ( $\bar{\mathbf{q}}_i$ ) and  $n$  by  $m$ . We will call these measures  $m$ -averaged measures and denote them by  $\bar{c}_mRMS$  and  $\bar{d}_mRMS$ .

Obviously, the error of these simplified similarity measures continuously approaches zero as the two compared point sets  $P$  and  $Q$  become more similar, i.e.  $\lim_{Q \rightarrow P} |\bar{c}_mRMS(P, Q) - cRMS(P, Q)| = 0$  and the same holds for  $\bar{d}_mRMS$ . For general point sets, the error introduced by this approximation can be quite substantial. However, for proteins the error is small because of their chain topology and because van der Waals forces limit the compactness of possible conformations. In the next section we will try to give an intuition as to why this is the case using random chains and wavelets analysis.

### 2.2 Random chains and Haar wavelets

In what follows we will use random chains and the Haar wavelet transform to argue that averaging is a reasonable method for reducing the size of the representation of a protein for computing structure similarities. A random chain  $C = (\mathbf{c}_0, \dots, \mathbf{c}_{n-1})$  in 3-D is an ordered set of points in space defined as follows:

$$\begin{aligned} \mathbf{c}_0 &= \mathbf{0}, \\ \mathbf{c}_{i+1} &= \mathbf{c}_i + \mathcal{S}_2 \cdot l \quad i = 0, \dots, n-2 \end{aligned} \quad (5)$$

where  $\mathcal{S}_2$  is a random 3-D vector uniformly distributed on the unit 3-D sphere and  $l$  is the fixed Euclidean distance between two consecutive points of the chain.  $\mathcal{S}_2$  is sampled as follows:

$$\mathcal{S}_2 = \begin{bmatrix} \sin \phi \cos \theta \\ \sin \phi \sin \theta \\ \cos \phi \end{bmatrix} \quad (6)$$

where  $\theta \sim U[0, 2\pi]$  and  $\cos \phi \sim U[-1, 1]$ . While it is a well-known fact that the positions of neighboring  $C_\alpha$  atoms along

the backbone of native protein structures are highly correlated (e.g., see [22]), it was shown in [18] that treating the position of each  $C_\alpha$  atom as uniformly distributed on a 3-D sphere centered at the center of the previous  $C_\alpha$  atom yields a very good approximation of the average global behavior of native protein structures.

Computing the covariance matrix of  $\mathcal{S}_2$  reveals that the off-diagonal elements are identically 0, and as a result the three dimensions of each random step are uncorrelated. Since each step is independent of all other steps the distributions of the three dimensions of any point on the chain are uncorrelated. Consequently, the random chain as described above can be approximated well by replacing  $\mathcal{S}_2$  with a 3-vector sampled from the normal distribution  $\mathcal{N}(\mathbf{0}, \frac{1}{3} \cdot \mathcal{I})$  (where  $\mathcal{I}$  is the  $3 \times 3$  identity matrix) when  $n > 10$ . Moreover, the fact that the three dimensions are uncorrelated allows us to perform three independent one-dimensional Haar wavelet transforms as described below instead of the more complicated three-dimensional transform.

The Haar wavelet transform of a chain is a recursive averaging and differencing of the coordinates of the points. The transform recursively smoothes the chain while keeping the *detail* coefficients needed to reconstruct the full chain from the smoothed out version. We define the full resolution chain to be of level 0:  $C = C^0$ . We recursively create smoothed versions of the chain by averaging pairs of consecutive points:

$$\mathbf{c}_i^j = \frac{1}{\sqrt{2}} \left( \mathbf{c}_{2i}^{j-1} + \mathbf{c}_{2i+1}^{j-1} \right) \quad \left\{ \begin{array}{l} j = 1, \dots, \log n \\ i = 0, \dots, \frac{n}{2^j} - 1 \end{array} \right. \quad (7)$$

As each level of resolution is created we also compute the *details* that are smoothed out by the averaging:

$$\mathbf{d}_i^j = \frac{1}{\sqrt{2}} \left( \mathbf{c}_{2i}^{j-1} - \mathbf{c}_{2i+1}^{j-1} \right) \quad \left\{ \begin{array}{l} j = 1, \dots, \log n \\ i = 0, \dots, \frac{n}{2^j} - 1 \end{array} \right. \quad (8)$$

Note that the averages and details are multiplied by a scale factor of  $\sqrt{2}$  at each level. Given  $C^j$ , the smoothed chain at level  $j$ , and  $D^j$ , the detail coefficients of level  $j$ , it is possible to reconstruct exactly  $C^{j-1}$  by inverting the formulas of Equations 7 and 8. The Haar wavelet transform of a chain  $C$  is thus defined as:

$$\hat{C} = \left( C^{\log n}, D^{\log n}, D^{\log n-1}, \dots, D^1 \right). \quad (9)$$

The length of  $\hat{C}$  is the same as  $C$  and  $C^{\log n}$  is the centroid of the entire chain. Since  $C$  can be exactly reconstructed from  $\hat{C}$ , no information is lost during the transform. This representation can then be compressed by removing (setting to 0) all coefficients in  $\hat{C}$  smaller than some threshold. Since the coefficients are scaled, the square of the  $L_2$  error of approximation in this case would be equal to the sum of the squares of the removed coefficients [36].

Given the normal approximation of the random chain construction, we can analytically determine the *pdf* (probability density function) of each of the coefficients in  $\hat{C}$  by adding, subtracting and scaling independent normally distributed variables. The *pdf* of each detail coefficient in level  $j$  can be derived as:

$$\mathbf{d}^j \sim \mathcal{N} \left( \mathbf{0}, \frac{4^j + 2}{36} \cdot \mathcal{I} \cdot l \right), \quad (10)$$

and the *pdf* of their squared  $L_2$  norm is thus:

$$\|\mathbf{d}^j\|_2^2 \sim \chi^2(3dof) \cdot \frac{4^j + 2}{36} \cdot l \quad (11)$$

with a mean of  $\frac{4^j + 2}{12} \cdot l$  and variance of  $\frac{(4^j + 2)^2}{216} \cdot l^2$ . Since the *pdfs* of the detail coefficients are centered at the origin and their variance is decreasing by a factor of roughly 4, they are expected to be ordered (in absolute value) in  $\hat{C}$ , from largest to smallest. Note that the  $\sqrt{2}$  scaling during the construction of the coefficients would account for an average growth of a factor of 2 in their variance from one level to the next. The special structure of random chains accounts for the second factor of 2. Hence, as a general policy, it is best to remove coefficients starting at the lowest level and climbing up. These coefficients have the lowest variance and thus contain the least information for determining structural similarity. The effect of averaging as described in Section 2.1 for  $m = 2^v$  is the same as that of removing the lowest  $(\log n) - v$  levels of coefficients. Since these are expected to be the smallest coefficients, we can conclude that using an  $m$ -averaged chain will give the smallest expected error for a representation that uses only  $m$  Haar detail coefficients for each dimension. The wavelet analysis allows us to estimate the approximation mean squared (MS) error introduced by removing all coefficients of level  $j$ . It can be computed to be  $\frac{l}{12} \left( 2^j + \frac{1}{2^{j-1}} \right)$ . Therefore for an  $m$ -averaged approximation the MS error is expected to be on the order of  $(n \cdot l)/(6m)$ .

As the above analysis shows, we can remove quite a few levels of coefficients without introducing a large error. This is due to the large *ratio of the average variances* (henceforth called RAV) between two successive levels of detail coefficients, which was shown to be approximately 4 for all levels. This behavior of the Haar detail coefficients is a result of the fact that we are dealing with chains that on the average grow further and further away from their starting point. The expected distance of the  $n$ th point from the origin is on the order of  $\sqrt{n} \cdot l$ . We see this behavior in Figure 1 where we compare the average variances of the coefficients of random chains to those of very compact random chains (chains forced to reside inside small spheres) and to those of point clouds sampled randomly from inside a sphere of radius  $\sqrt{n} \cdot l$ . All chains are of length  $n = 64$ . The RAV of the unconstrained random chain is significantly larger than that for the compact random chains, which decreases as the compactness of the chain is increased. The worst case is for a point cloud, where the average variances of all levels of detail coefficients have the same magnitude making all levels have the same importance.

We performed the same wavelet transform on sets of conformations of actual proteins of length 64 residues (only the  $C_\alpha$  atoms) taken from *decoy sets* (conformations which are expected to be similar to the native conformation) generated by Park and Levitt [28], containing 10,000 conformations each. We obtained results similar to those of random chains, namely the detail coefficients are ordered and have a RAV similar to that of random chains. The results for a few sets of proteins are presented in Figure 2. One important difference from random chains is that the RAV for decoy sets decreases considerably for the top levels. We explain this as follows. Small pieces of a protein cannot be highly packed because of steric clashes, while intermediate size pieces are often elongated (secondary structure helices and strands) and hence the variance of the coefficients grows considerably from one level to the next at the low and intermediate levels. The tight packing of the secondary structure of the native-like conformations makes the high-level coeffi-

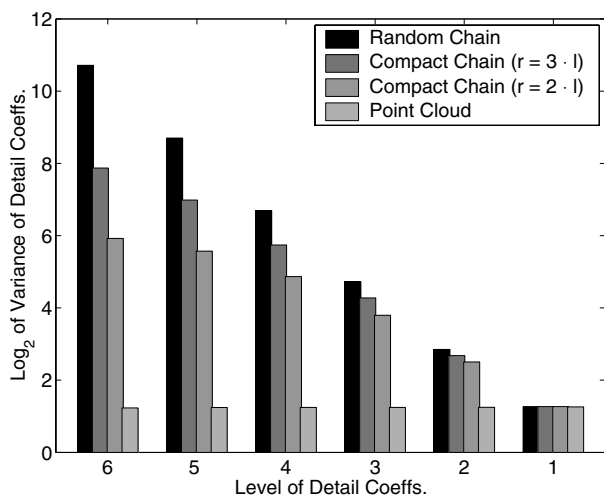


**Figure 1: Comparison of the average variance of Haar coefficients of random chains, compact random chains and random point clouds.**

coefficients considerably smaller than in the random chain model. We would have liked to give results for decoy sets of proteins longer than 64 residues, however, no such sets were available to us.

Random protein conformations (generated as described in Section 2.3), on the other hand, are considerably less compact than the decoy sets, and hence behave much more like random chains at *all* levels of detail coefficients. As can be seen in Figure 2 the RAV at the lower levels is even bigger than what is observed for random chains. This is due to the limit on the packing density as a result of the space taken up by each residue. In our random chain model the points have no volume and the chain is allowed to cross itself. In the random protein conformations, however, atoms are not allowed to have any self-overlaps. Their behavior is actually modelled better by random chains in which the next step is sampled uniformly from a *hemisphere* defined by the direction of the previous step.

We thus conclude that, while decoy sets cannot be compressed as much as random sets, it is possible to remove the first few levels and still get a very good approximation.

### 2.3 Correlation of approximate and exact similarity measures

When using the *cRMS* measure to compute similarity between random chains of length 64 we find that the approximate *m*-averaged versions yield very good results for *m* as small as 8. For *m* = 4, 8, 12 and 20, Pearson’s correlation of the approximate measure to the true one is 0.59, 0.92, 0.97 and 0.99, respectively. When using the *dRMS* measure to compute similarity between random chains the approximate *m*-averaged versions is highly correlated for *m* as small as 12. The correlation values obtained are 0.45, 0.78, 0.88 and 0.94, respectively.

In order to verify that the analogous behavior of the detail coefficients of protein sets and random chains carries over to approximate similarity measures we chose 9 structurally diverse proteins used by Park and Levitt in [28] (1CTF, 1ERP, 1R69, 1SN3, 1UBQ, 2CRO, 3ICB, 4PTI, 4RXN) having be-

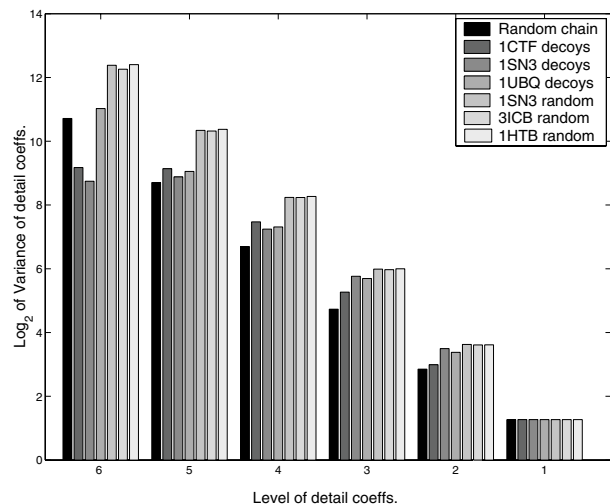


**Figure 2: Comparison of the Haar coefficients of decoy sets of protein and randomly generated conformations of proteins to the coefficients of a set of random chains.**

tween 38 and 76 residues. For these proteins we obtained (1) decoy sets generated by Park and Levitt, containing 10,000 conformations each and (2) randomly generated conformation sets using the program FOLDTRAJ<sup>1</sup> [9], containing 5000 structures each.

For each set, we randomly chose between 1000 and 4000 pairs whose true *dRMS* distance was less than 5Å and computed their *m*-averaged distances for different values of *m*. The correlation of the *m*-averaged *cRMS* and *dRMS* measures to the true *cRMS* and *dRMS* measures for the different decoy sets can be found in Table 1(a). For *m* = 8, the approximate *cRMS* measure is already highly correlated with the true *cRMS* measure, which means that a reduction factor between 5 and 8 still yields a very good approximation. For *dRMS*, high correlation is achieved for *m* = 12, which means a reduction factor of between 3 and 6 (since the complexity of *dRMS* is quadratic, the actual gain is by a factor of between 9 and 36). We note that the correlation values obtained are quite similar to those computed for random chains.

The correlation of the *m*-averaged *cRMS* and *dRMS* measures to the true measures for the different random sets can be found in Table 1(b). Here too, a reduction factor between 5 and 8 yields a highly correlated approximation of the *cRMS* measure. For *dRMS*, high correlation is achieved for *m* = 8, which means a reduction factor between 5 and 8 (i.e., an actual gain between 25 and 64). Here the correlation values are in fact better than those computed for random chains as would be anticipated from the higher growth ratio of the variance of the detail coefficients of random protein sets in comparison to those of random chains (see Figure 2). By examining all pairs (not only those whose *dRMS* distance is smaller than 5Å), the Pearson’s correlation is even larger.

<sup>1</sup><http://bioinfo.mshri.on.ca/trades/>

m	1CTF		1ERP		1R69		1SN3		1UBQ		2CRO		3ICB		4PTI		4RXN	
	<i>cRMS</i>	<i>dRMS</i>	<i>cRMS</i>	<i>dRMS</i>	<i>cRMS</i>	<i>dRMS</i>	<i>cRMS</i>	<i>dRMS</i>	<i>cRMS</i>	<i>dRMS</i>	<i>cRMS</i>	<i>dRMS</i>	<i>cRMS</i>	<i>dRMS</i>	<i>cRMS</i>	<i>dRMS</i>	<i>cRMS</i>	<i>dRMS</i>
4	0.38	0.42	0.88	0.86	0.64	0.47	0.54	0.45	0.37	0.47	0.73	0.52	0.57	0.40	0.42	0.46	0.49	0.49
8	0.90	0.77	0.97	0.94	0.97	0.87	0.94	0.78	0.84	0.70	0.97	0.89	0.98	0.86	0.95	0.83	0.93	0.79
12	0.98	0.93	0.98	0.96	0.99	0.92	0.98	0.94	0.98	0.92	0.99	0.95	0.99	0.92	0.98	0.92	0.98	0.94
16	0.99	0.95	0.99	0.98	0.98	0.92	0.99	0.97	0.98	0.95	0.99	0.97	0.98	0.92	0.98	0.94	0.98	0.97
20	0.99	0.96	0.98	0.96	0.99	0.96	0.99	0.97	0.99	0.96	0.99	0.97	0.98	0.93	0.99	0.95	0.98	0.95

(a)

m	1CTF		1ERP		1R69		1SN3		1UBQ		2CRO		3ICB		4PTI		4RXN	
	<i>cRMS</i>	<i>dRMS</i>	<i>cRMS</i>	<i>dRMS</i>	<i>cRMS</i>	<i>dRMS</i>	<i>cRMS</i>	<i>dRMS</i>	<i>cRMS</i>	<i>dRMS</i>	<i>cRMS</i>	<i>dRMS</i>	<i>cRMS</i>	<i>dRMS</i>	<i>cRMS</i>	<i>dRMS</i>	<i>cRMS</i>	<i>dRMS</i>
4	0.69	0.59	0.85	0.92	0.68	0.65	0.68	0.63	0.65	0.53	0.70	0.64	0.65	0.55	0.72	0.71	0.73	0.74
8	0.96	0.90	0.99	0.99	0.97	0.93	0.97	0.92	0.96	0.84	0.97	0.91	0.96	0.86	0.97	0.95	0.97	0.96
12	0.99	0.97	0.99	0.98	0.99	0.97	0.99	0.97	0.99	0.95	0.99	0.97	0.99	0.95	0.99	0.98	0.99	0.98
16	0.99	0.98	0.99	0.99	0.99	0.99	0.99	0.99	0.99	0.97	0.99	0.99	0.99	0.97	0.99	0.98	0.99	0.98
20	0.99	0.98	0.97	0.96	0.99	0.98	0.99	0.98	0.99	0.97	0.99	0.98	0.99	0.97	0.99	0.98	0.99	0.97

(b)

**Table 1: Pearson’s correlation coefficient for different  $m$  values evaluated for  $cRMS$  and  $dRMS$  of (a) decoy sets and (b) randomly sampled conformations of various proteins.**

### 3. APPLICATION 1: NEAREST-NEIGHBOR SEARCH

Simulations and other conformational sampling methods generate large sets of conformations of a particular protein. For example, the project Folding@Home<sup>2</sup> runs parallel molecular dynamics simulations on several thousands of computers across the Internet and then centrally evaluates the obtained data. An important step in evaluating such data, e.g. for clustering and related tasks, is the following: given a set of conformations of the same protein, find the  $k$  nearest neighbors (NNs) for each sample in the set. Typically,  $k$  is a small constant while the size of the set can be very large.

The straightforward (“brute-force”) approach is to evaluate the similarity measure ( $cRMS$  or  $dRMS$ ) for all pairs and then report the  $k$  NNs for each sample. However, the quadratic complexity makes this approach scale badly. Spatial data structures such as the *kd-tree* [4] can avoid this complexity under certain circumstances [1, 7, 17, 19, 25, 29]. Note that these data structures allow for exact search, i.e., they return the same NNs as would the brute-force search. However, most of them require a Euclidean metric space of rather small dimensionality. Unfortunately,  $cRMS$  is not a Euclidean metric. Although  $dRMS$  is a Euclidean metric, the dimensionality of the space of intra-molecular distance matrices is far too high. (Typically, for dimensions higher than a few tens, none of the nearest-neighbor data structures performs better than brute-force search.) Therefore, if we hope to use a spatial data structure to speed up NNs search, we must use the  $dRMS$  measure, but find a way to significantly reduce the dimensionality of the structure descriptors below the averaged conformations we presented in Section 2.

#### 3.1 Further reduction of distance matrices

We use singular value decomposition (SVD) [14] to further compress the intra-molecular distance matrices of averaged proteins, that is to further reduce the number of parameters involved in computing  $\bar{d}_m RMS$ . SVD is a standard tool for principal components analysis (PCA) and computes

<sup>2</sup><http://folding.stanford.edu>

directions of greatest variance (and thus distance information) in a given set of high-dimensional points. These directions are called principal components (PCs). The SVD can be used to linearly map a set of high-dimensional input vectors (data points), stored in a matrix  $A$ , into a lower-dimensional subspace while preserving most of the variance. Such a transform can be found by decomposing the matrix  $A$  of the input vectors into  $A = USV^T$ , the SVD of  $A$ , where  $U$  and  $V$  are orthogonal matrices and  $S$  is diagonal with the singular values of  $A$  along the diagonal.

Efficient algorithms exist that compute the SVD in time  $O(s^2t)$  where  $s$  is the smaller and  $t$  the larger dimension of  $A$  (rows or columns). Note that while in principle, SVD could be applied to intra-molecular distance matrices without first averaging protein pieces, the quadratic dependency on the smaller dimension of  $A$  shows the important advantage of averaging: usually, the larger dimension  $t$  will reflect the size of the conformational sample set while the smaller dimension  $s$  will correspond to the size of a single intra-molecular distance matrix. Reducing the distance matrix size by using averaged conformations, as described in Section 2, is therefore key to performing SVD in practice.

To perform SVD on a set of intra-molecular distance matrices derived from  $m$ -averaged conformations, each of these distance matrices is rewritten as an  $m(m-1)/2$  dimensional vector and then SVD is applied to the matrix that contains all these vectors. Taking the resulting  $U$  matrix and removing all columns that correspond to small singular values (the directions of little variance), we have the linear map that takes the set of distance matrices into a lower-dimensional Euclidean space while preserving a high percentage of the variance and thus distance information. We found that in practice, a relatively small output dimensionality between 10 and 20 is sufficient to maintain about 90% of the variance of the distance matrices.

In the following, we will denote the  $dRMS$  measure obtained from an SVD compressed set of  $m$ -averaged distance matrices by  $\bar{d}_m^{PC} RMS$ . ( $PC$  stands for the number of principal components that are used after compression.)

#### 3.2 Evaluation of approximation errors

Of course, by reducing the dimensionality of distance ma-

	$k = 10$		$k = 25$		$k = 100$	
	$E_1$	$E_2$	$E_1$	$E_2$	$E_1$	$E_2$
1CTF	1.1	1.04	1.116	1.036	1.104	1.023
1ERP	1.3	1.158	1.292	1.124	1.246	1.083
1R69	1.201	1.093	1.192	1.074	1.165	1.048
1SN3	1.161	1.086	1.155	1.063	1.136	1.04
1UBQ	1.199	1.105	1.184	1.08	1.162	1.045
2CRO	1.118	1.061	1.155	1.056	1.141	1.041
3ICB	1.152	1.054	1.154	1.048	1.129	1.033
4PTI	1.186	1.099	1.188	1.079	1.17	1.055
4RXN	1.179	1.079	1.186	1.072	1.163	1.046

**Table 2: Mean errors  $E_i = E(err_i)$  for 100 queries of  $k$  nearest neighbors. Park-Levitt decoys, 20 PCs.**

	$k = 10$		$k = 25$		$k = 100$	
	$E_1$	$E_2$	$E_1$	$E_2$	$E_1$	$E_2$
decoys	1.337	1.248	1.34	1.196	1.347	1.141
decoys2	1.136	1.052	1.171	1.049	1.158	1.036
uniform	1.101	1.035	1.107	1.029	1.113	1.02

**Table 3: 1CTF: Mean errors  $E_i = E(err_i)$  for 100 queries of  $k$  nearest neighbors. Decoys, decoys2: 100,000 decoys from Park-Levitt set ( $m = 16$  and 20 PCs). Decoys2: excluding 8 outliers. Uniform: 100,000 uniformly sampled conformations ( $m = 16$  and 16 PCs).**

trix space from  $dRMS$  over  $\bar{d}_mRMS$  to finally  $\bar{d}_m^{PC}RMS$ , we lose some information. However, we observed that in general, the introduced errors are small enough to allow for good results in finding most of the true  $k$  nearest neighbors. In what follows, we illustrate this with different error measures.

For a set of conformations  $S$  and a given query conformation  $Q$  from that set, we define two subsets  $S_1$  and  $S_2$  of size  $k$  each.  $S_1$  is the set of  $k$  nearest neighbors of  $Q$  in  $S$  using exact  $dRMS$ .  $S_2$  is the set of  $k$  nearest neighbors of  $Q$  in  $S$  using  $\bar{d}_m^{PC}RMS$ . Thus,  $S_2$  is the approximation of  $S_1$  using our reduced similarity measure.

In a first experiment, we evaluated how many of the exact  $k$  nearest-neighbor conformations in  $S_1$  are contained in  $S_2$  as well. To this end, we looked at the  $k = 100$  nearest neighbors for each of 100 query conformations and computed the average number of such matches over the 100 queries. Using  $\bar{d}_{16}^{20}RMS$  on sets  $S$  of 10,000 decoys of 1R69, 4PTI, 2CRO, 1SN3 and 3ICB, these averages ranged from 74.8 to 83.3 (roughly 80 on average). Using  $\bar{d}_{16}^{18}RMS$  on sets  $S$  of 5,000 uniform samples of the same proteins, corresponding averages were between 86.1 and 94.2 (about 90 on average). These results show that, using our approximations, not too many extra samples would have to be drawn in order to obtain sufficiently many exact nearest neighbors.

However, in cases in which significantly more than  $k$  conformations are clustered around the query conformation, the number of identical matches may not be a good quality measure. In such cases, it may even be possible to obtain a very different candidate set with almost the same distribution of distances from the query conformation. We therefore used the two following error measures to further evaluate the quality of our approximations.

**err<sub>1</sub>** The ratio of the exact  $dRMS$  of the furthest conformation in  $S_2$  to the exact  $dRMS$  of the furthest conformation in  $S_1$ .

**err<sub>2</sub>** The ratio of the average exact  $dRMS$  of all conformations in  $S_2$  to the average exact  $dRMS$  of all conformations in  $S_1$ .

We first looked at the decoy sets of size 10,000 for each of the nine Park-Levitt proteins. We used  $m = 16$  and 20 PCs. For each set, we randomly chose 100 query conformations and evaluated  $err_1$  and  $err_2$  for each of them. Table 2 shows the means  $E_i = E(err_i)$  of both errors over the 100 queries (standard deviations were generally small). The mean error  $E_1$  is usually noticeably smaller than 1.2 which means that the worst-case error by our reduction is smaller than 20%. The mean error  $E_2$  is almost always noticeably smaller than 1.1 indicating an average error of less than 10%. Note that these percentages correspond to small absolute values of about 1.5Å and 0.7Å, respectively.

We also evaluated the error measures for two large sets of 100,000 conformations of 1CTF, a decoy set and a uniformly sampled set. Here, we used  $m = 16$  and 20 PCs for the decoys and  $m = 16$  and 16 PCs for the uniform samples. The results are presented in Table 3. For the decoys we noticed both errors to be slightly higher than for the smaller data set above. However, when we ignore 8 out of the 100 query conformations, which were obvious outliers, we got comparable results (row labelled *decoys2*). For the uniform samples, both relative errors were significantly smaller than for the decoy set.

### 3.3 Running time

We now consider the running times in a concrete nearest-neighbor task: given a set of 100,000 random conformations of protein 1CTF, find  $k = 100$  nearest neighbors for each sample in the set. The reported times in this section refer to a sequential implementation in C running on a single 1GHz Pentium processor on a standard desktop PC.

We first compare the running times for a brute-force (all-pairs) implementation using both  $cRMS$  and  $dRMS$ , and their corresponding averaged similarity measures  $\bar{c}_mRMS$  and  $\bar{d}_mRMS$ . Table 4 shows that the latter measures already result in a notable speed-up. For  $\bar{d}_{16}RMS$ , a significant speed-up over  $dRMS$  is obtained due to the quadratic down-scaling of intra-molecular distance matrices by averaging proteins. For  $\bar{c}_{16}RMS$ , the improvement over  $cRMS$  is smaller. This is because the reduction by averaging affects the number of involved points only linearly, and the main effort in computing  $cRMS$  comes from finding an optimal rigid-body alignment of two point sets.

Note that the increase in running times agrees quite well with the expected quadratic scaling of the brute-force nearest neighbor approach. The times for  $N = 100,000$  samples were therefore extrapolated from the actual running times measured for the smaller values of  $N$ . In fact, for  $dRMS$  using all  $C_\alpha$  atom coordinates, we had problems storing all intra-molecular distance matrices (however, these problems do not occur with averaged proteins and  $\bar{d}_mRMS$ ).

We next address the quadratic scaling problem of the brute-force approach. To be able to apply a kd-tree, we first further reduced the 120-dimensional space of  $\bar{d}_{16}RMS$  using SVD and retained 16 principal components. This further compression took about one minute for the complete

$N$	$cRMS$	$\bar{c}_{16}RMS$	$dRMS$	$\bar{d}_{16}RMS$
1,000	18.6s	12.4s	31.0s	2.2s
2,000	74.4s	50.0s	137.5s	8.0s
5,000	464.8s	312.0s	759.8s	43.4s
100,000	~52h	~35h	~84h	~4.8h

**Table 4: Brute-force search using  $cRMS$  vs  $\bar{c}_{16}RMS$  and  $dRMS$  vs  $\bar{d}_{16}RMS$  for finding the  $k = 100$  nearest neighbors for each of  $N$  samples.**

k	Brute-force	kd-tree
1	30min	4min10sec
100	41min	19min

**Table 5: Brute-force vs kd-tree search for  $k$  nearest neighbors for each of 100,000 samples. Used similarity measure:  $\bar{d}_{16}^{16}RMS$ .**

set of 100,000 samples. Building the kd-tree for the resulting 16-dimensional data took only about 4 seconds. The correlation coefficient of the resulting  $\bar{d}_{16}^{16}RMS$  and  $dRMS$  was found to be still about 0.94. As reported in the previous section, the approximation errors are also low (Table 3).

We then ran both the brute-force and the kd-tree approach using  $\bar{d}_{16}^{16}RMS$  as similarity measure. Table 5 shows the running times for finding  $k = 1$  and  $k = 100$  nearest neighbors for each sample in the full set of 100,000 samples. The obtained total speed-up of our nearest-neighbor search (approximate similarity measures and a kd-tree) over the current best approach (brute-force search using all  $C_\alpha$  coordinates) is several orders of magnitude.

In general, the speed-up obtained by using a kd-tree can be expected to increase with increasing sample set size  $N$ . Due to its quadratic scaling, brute-force search will become very slow for larger sample sets. On the other hand, the sub-quadratically scaling kd-tree approach should allow to process even much larger sample sets within a few hours without parallelization on a standard desktop PC.

## 4. APPLICATION 2: STRUCTURAL CLASSIFICATION

Given a set of native protein structures each having a different amino-acid sequence, such as the Protein Data Bank (PDB)<sup>3</sup> [5], we would like to automatically classify the structures into groups according to their structural similarity. This task has been performed manually in the SCOP (structural classification of proteins) database<sup>4</sup> [26], where protein structures are hierarchically classified into *classes*, *folds*, *superfamilies* and *families*. The major difficulty in performing this classification automatically lies in the need to decide, given two protein structures, which parts of both structures should be compared, before it can be determined how similar these parts are. This *correspondence problem* does not arise when different conformations of the same protein are compared because in that case the correspondence is trivially determined. For this reason, computing the similarity between structures of different proteins requires considerably more computation than the methods described in Section 2.

Several algorithms have been proposed for structural clas-

sification. The DALI<sup>5</sup> method [15] starts with the distance matrices of both proteins. It finds all pairs of similar sub-matrices of small fixed size (one from each protein distance matrix) and then uses a Monte Carlo algorithm to assemble the pairs into larger consistent alignments. The PROSUP<sup>6</sup> method [23] initially identifies similar fragments in both proteins and iteratively expands them to create alignments. A dynamic algorithm is then used to iteratively refine each alignment and finally insignificant alignments are removed. The CE<sup>7</sup> algorithm [30] cuts each structure into small fragments and creates a matrix of all possible aligned fragment pairs (AFPs). Combinations of AFPs are selectively extended and discarded leading to a single optimal alignment. The STRUCTAL<sup>8</sup> method [11] directly matches the backbones of the two protein structures by iteratively cycling between a dynamic programming algorithm and least-square fitting to come up with an alignment that minimizes coordinate difference. For other methods see [20].

### 4.1 The modified STRUCTAL algorithm

All the above methods stand to gain in performance by using our averaging scheme. In order to verify this claim, we tested the speedup and accuracy obtained by using the STRUCTAL method on averaged protein structures. We could not test our approach on PROSUP, DALI and CE because both servers did not accept our averaged structures because they are not valid protein structures, and the algorithms were too involved for us to implement ourselves reliably.

The STRUCTAL algorithm starts with an initial alignment of the backbone  $C_\alpha$  atoms of the two structures according to one of a number of possible heuristics (aligning the beginnings, the ends, random segments, by sequence similarity, etc). Then a two step process is repeated until convergence. First a dynamic programming algorithm based on the Needleman and Wunsch sequence alignment algorithm [27] finds the correspondence between the two structures that yields the highest score. Scoring is based on assigning a cost to each possible corresponding pair, which is inversely proportional to the distance between  $C_\alpha$  positions, and a gap penalty for every gap in the alignment. Computing the best correspondence thus requires  $O(n_1n_2^2 + n_2n_1^2)$  time ( $n_1$  and  $n_2$  are the number of residues in each structure). Second, an optimal alignment is computed based on the best correspondence using the method in [16]. The  $cRMS$  distance of the final alignment and the number of corresponding residues is returned as a measure of the similarity of the two structures. Since the result is sensitive to the initial alignment, the algorithm is usually run a number of times for each pair of structures, each time using a different initial alignment. The best (smallest) result of all the runs is kept.

By combining averaging with this algorithm, we add another degree of freedom to the computation. If we average each  $r$  successive  $C_\alpha$  atom positions, we have a choice of  $a = \text{mod}(n_1, r)$  positions to start the averaging process for one structure and  $b = \text{mod}(n_2, r)$  for the other. As a result, there are  $a \times b$  possible pairs of averaged structures that could possibly result in different alignment scores. Therefore, more runs per pair of structures would be necessary

<sup>5</sup><http://www2.ebi.ac.uk/dali>

<sup>6</sup>[http://lore.came.sbg.ac.at/CAME/CAME\\_EXTERN/PROSUP](http://lore.came.sbg.ac.at/CAME/CAME_EXTERN/PROSUP)

<sup>7</sup><http://cl.sdsc.edu/ce.html>

<sup>8</sup><http://bioinfo.mbb.yale.edu/align>

<sup>3</sup><http://www.rcsb.org/pdb/>

<sup>4</sup><http://scop.mrc-lmb.cam.ac.uk/scop/>

when using our averaging scheme. However, the gain from averaging stands to be very large. Since both  $n_1$  and  $n_2$  are reduced by a factor of  $r$ , the complexity of the dynamic programming, which is the main part of the algorithm, is reduced by a factor of  $r^2$ .

## 4.2 Experimental results

We implemented the STRUCTAL algorithm as described in [11]. Our implementation initially aligns the two structures by choosing a random correspondence. Therefore, we ran the algorithm 12 times for every pair of structures and kept the smallest result as the similarity score. In [11] they run the algorithm a few times as well, using a number of different initial alignment heuristics.

We used two data sets to test the modified STRUCTAL. We queried the ASTRAL database<sup>9</sup> [6] for all protein domains which have less than 40% sequence similarity. This yielded 4772 structures. We then took (from this large set) all superfamilies (as defined by SCOP), which had more than 40 structures, and with sequence length between 100 and 400 residues. We got 5 superfamilies having between 40 and 104 structures each. We will refer to this set as set *A* and use it to test the performance of modified STRUCTAL within superfamilies. We also randomly chose 25 superfamilies from the large set and from each took 12 structures at random to create set *B*, which has 300 structures altogether. All members of this set have sequence length between 100 and 300 residues. This second set will be used to test the modified STRUCTAL on a heterogenous set of structures.

We computed the similarity between all pairs of structures inside each of the five superfamilies in set *A*. We computed the similarity using the STRUCTAL algorithm and then computed approximate similarity using the modified STRUCTAL with  $r = 3, 5$  and  $8$ . Modified STRUCTAL was run 18 times for  $r = 3$ , 24 times for  $r = 5$  and 40 times for  $r = 8$ . We then counted how many out of the 7 real nearest neighbors of a structure (as computed by STRUCTAL) are present in the set of  $q$  nearest neighbors computed by the modified STRUCTAL. This would tell us how good the modified STRUCTAL is as a pre-filter for finding real nearest neighbors. The results for  $q = 7, 14$  and  $21$  are found in Table 6. The results for the first two superfamilies *C.1.8* and *C.3.1* are good. When  $q = 14$  more than  $3/4$  of the real nearest neighbors are found for  $r = 3$ , and more than  $2/3$  are found for  $r = 5$ . For the other three superfamilies the results are not as good. For *B.1.1* and *C.2.1*, when  $q = 14$ , about  $2/3$  of the real nearest neighbors are found for  $r = 3$ , and less than  $3/5$  are found for  $r = 5$ . For *C.37.1* the results are even worse. The speedup of the modified STRUCTAL over STRUCTAL is a factor of 7 for  $r = 3$ , a factor of 19 for  $r = 5$  and 46 for  $R = 8$ .

For set *B* we computed the similarity between all pairs of structures in the set using STRUCTAL and using the modified STRUCTAL with  $r = 3, 5$  and  $8$  (in the same manner as for set *A*). The results for  $q = 7, 14$  and  $21$  are found in Table 7. Using the modified STRUCTAL with ( $q = 14$ ), less than half of the 7 true nearest neighbors were found when  $r = 3$  and about a third were found when  $r = 5$ . The results improve when we restrict the analysis to pairs of structures where the correspondence of the similarity (the number of corresponding atoms for the two compared structures) is above some threshold. In Table 7 this threshold

<sup>9</sup><http://astral.stanford.edu>

was set to 100, 150 and 200 residues. Clearly as the size of the correspondence increases so does the ability of modified STRUCTAL to pick out the true nearest neighbors.

The Pearson correlation between the similarity score computed by STRUCTAL and the score computed by the modified STRUCTAL, for both data sets is reported in Table 8. The correlation for the 5 superfamilies of set *A* is in part (a). These correlation values are low compared to the correlations reported in Section 2.3, which explains why the performance of the modified STRUCTAL in picking out nearest neighbors is not as good as that of the averaging scheme reported in Section 3.2. Part (b) of Table 8 reports the correlation for set *B* using a number of thresholds on the size of the correspondence. Although the correlation is pretty high, these results are misleading. They contain many pairs of structures which are very dissimilar and thus their similarity score is meaningless (see [11]). These large scores bias the correlation upward, and hide the fact that the correlation is poorer when the score is low.

superfamily	$r = 3$	$r = 5$	$r = 8$
C.1.8	0.60	0.44	0.35
C.3.1	0.62	0.56	0.56
B.1.1	0.55	0.52	0.54
C.2.1	0.66	0.58	0.56
C.37.1	0.61	0.57	0.57

(a)

CRSP	$r = 3$	$r = 5$	$r = 8$
$\geq 0$	0.85	0.75	0.66
$\geq 100$	0.86	0.76	0.66
$\geq 150$	0.84	0.71	0.60
$\geq 200$	0.54	0.30	0.17

(b)

**Table 8: The correlation of the similarity measure computed by STRUCTAL and these computed by the modified STRUCTAL. In (a) are the results for the 5 superfamilies of set *A*, and in (b) the results for set *B* using different correspondence size thresholds.**

In summary, although the modified STRUCTAL is significantly faster than STRUCTAL, the results it generates are disappointing and not reliable enough to warrant using it as a pre-filter for classifying a heterogenous set of protein structures, unless only a small number of nearest neighbors are required. It is more reliable for structures that belong to the same superfamily, or that are expected to have a large correspondence size.

## 5. CONCLUSION

Two general properties of proteins, their chain topology and limited compactness, are exploited to uniformly reduce the number of features for structural similarity computations. Substantial savings in terms of storage and running time are attained with small errors.

In applications in which no approximation error is tolerable, our approach can be used as a first step to filter a small subset of pairs that are within some tolerance band around the desired similarity. More expensive exact similarity measures can then be used on the reduced set of pairs.

#ANN	C.1.8 (40)			C.3.1 (41)			B.1.1 (79)			C.2.1 (89)			C.37.1 (104)		
	$r=3$	$r=5$	$r=8$	$r=3$	$r=5$	$r=8$	$r=3$	$r=5$	$r=8$	$r=3$	$r=5$	$r=8$	$r=3$	$r=5$	$r=8$
q=7	4.05	3.33	2.88	3.66	3.32	3.00	2.68	2.43	2.42	3.33	2.98	2.78	2.93	2.34	2.37
q=14	5.43	4.55	4.10	5.24	4.76	4.90	3.86	3.88	3.52	4.56	4.08	4.07	3.92	3.56	3.38
q=21	5.87	5.20	5.10	6.15	5.73	5.88	4.66	4.71	4.47	5.29	4.80	4.74	4.61	4.15	4.09

**Table 6:** The results for the 5 superfamilies in set *A*. The size of each superfamily is in parenthesis next to its name. This table presents the average number of real nearest neighbors (the 7 most similar structures) of each of the structures in each superfamily that appear in the list of approximate nearest neighbors of length  $q$  found by the modified STRUCTAL. #ANN stands for number of approximate nearest neighbors

#ANN	$CRSP \geq 0$ (300)			$CRSP \geq 100$ (252)			$CRSP \geq 150$ (59)			$CRSP \geq 200$ (7)		
	$r=3$	$r=5$	$r=8$	$r=3$	$r=5$	$r=8$	$r=3$	$r=5$	$r=8$	$r=3$	$r=5$	$r=8$
q=7	2.47	1.99	1.84	3.12	2.66	2.35	3.40	3.05	2.93	2.86	3.14	3.14
q=14	3.19	2.60	2.51	4.01	3.58	3.23	4.73	4.41	4.36	5.57	5.42	5.42
q=21	3.53	3.04	2.93	4.56	4.08	3.87	5.54	5.32	5.19	6.43	5.86	5.71

**Table 7:** The results for the structures in set *B*, where the size of the correspondence was taken into account. Only structures that have at least 35 nearest neighbors of the required correspondence size or larger are considered. Their number appears in parenthesis at the head of the column. For each correspondence size, we report the average number of real nearest neighbors (the 7 most similar structures) that appear in the list of approximate nearest neighbors of length  $q$  found by the modified STRUCTAL. #ANN stands for number of approximate nearest neighbors and  $CRSP$  is the size of the correspondence in each alignment of a pair of structures.

Two possible applications were presented: finding  $k$  nearest neighbors in large sets of conformations of the same protein and classification of different proteins using the STRUCTAL algorithm. For the first application the introduced error was low and the correlation to the true similarity measure was very high. For the second application the correlation to the true similarity measure was considerably lower and the error introduced by the reduction was quite high. Thus the usefulness of the reduction is limited in this case. In both applications, the running times were reduced from days to hours or even minutes.

In general, applications that input very large sets of proteins or that employ computationally intensive algorithms on large proteins stand to benefit from approximation of structures as suggested in this paper.

## 6. ACKNOWLEDGMENTS

The authors would like to thank Patrice Koehl, Pankaj Agarwal and Jean-Claude Latombe for comments and Patrice Koehl for providing the full Park-Levitt decoy set for the nearest-neighbor experiments. This work was partially funded by NSF ITR grant DUKE UNI/01-SC-NSF-1009-01 and a grant from Stanford’s Bio-X program.

## 7. REFERENCES

- [1] P. K. Agarwal. Range searching. In J. E. Goodman and J. O’Rourke, editors, *Handbook of Discrete and Computational Geometry*, pages 575–598. CRC Press, 1997.
- [2] M. S. Apaydin, D. L. Brutlag, C. Guestrin, D. Hsu, and J.-C. Latombe. Stochastic roadmap simulation: An efficient representation and algorithm for analyzing molecular motion. In *RECOMB*, pages 12 – 21, 2002.
- [3] M. S. Apaydin, A. P. Singh, D. L. Brutlag, and J.-C. Latombe. Capturing molecular energy landscapes with probabilistic conformational roadmaps. In *Proc. IEEE Intl. Conf. on Rob. and Autom.*, pages 932–939, 2001.
- [4] J. Bentley. multidimensional binary search trees used for associative searching. *commun. ACM*, 18:509 – 517, 1975.
- [5] H. Berman, J. Westbrook, Z. Feng, G. Gilliland, T. Bhat, and H. W. et al. The protein data bank. *Nucl. Acids Res.*, 28:235 – 242, 2000.
- [6] S. Brenner, P. Koehl, and M. Levitt. The ASTRAL compendium for sequence and structure analysis. *Nuclein Acids Research*, 28:254 – 256, 2000.
- [7] K. L. Clarkson. Nearest neighbor queries in metric spaces. In *Proc. 29th Annu. ACM Sympos. Theory Comput.*, pages 609–617, 1997.
- [8] B. Fain and M. Levitt. A novel method for sampling alpha-helical protein backbones. *J. Mol. Biol.*, 305:191–201, 2001.
- [9] H. J. Feldman and C. W. Hogue. A fast method to sample real protein conformational space. *Proteins*, 39(2):112–131, 2000.
- [10] Z. K. Feng and M. J. Sippl. Optimum superimposition of protein structures: ambiguities and implications. *Fold. Des.*, 1:123–132, 1996.
- [11] M. Gerstein and M. Levitt. Comprehensive assessment of automatic structural alignment against a manual standard, the scop classification of proteins. *Protein Science*, 7:445–456, 1998.
- [12] J. F. Gibrat, T. Madej, and S. H. Bryant. Surprising similarities in structure comparison. *Curr. Opin. Struct. Biol.*, 6(3):377–385, 1996.
- [13] A. Godzik. The structural alignment between two proteins: is there a unique answer? *Protein Sci.*, 5:1325–1338, 1996.
- [14] G. Golub and C. V. Loan. *Matrix Computations*. Johns Hopkins University Press, 3rd edition, 1996.
- [15] L. Holm and C. Sander. Protein structure comparison by alignment of distance matrices. *J. Mol. Biol.*, 233(1):123 – 128, 1993.
- [16] B. K. P. Horn. Closed form solution of absolute orientation using unit quaternions. *Journal of the*

- Optical Society A*, 4(4):629–642, April 1987.
- [17] P. Indyk. *High-dimensional Computational Geometry*. PhD thesis, Stanford University, September 2000.
- [18] K. Kedem, L. Chew, and R. Elber. Unit-vector RMS (URMS) as a tool to analyze molecular dynamics trajectories. *Proteins: Structure, Function and Genetics*, 37:554 – 564, 1999.
- [19] J. Kleinberg. Two algorithms for nearest-neighbor search in high dimension. In *Proc. 29th Annu. ACM Sympos. Theory Comput.*, pages 599–608, 1997.
- [20] P. Koehl. Protein structure similarity. *Current Opinion in Structural Biology*, 11:348–353, 2001.
- [21] P. Koehl and M. Delarue. Building protein lattice models using self-consistent mean field theory. *Journal of Chemical Physics*, 108(22):9540–9549, 1998.
- [22] R. Kolodny, P. Koehl, L. Guibas, and M. Levitt. Small libraries of protein fragments model native protein structures accurately. *J. of Mol. Biol.*, 323(2):297 – 307, Oct 2002.
- [23] P. Lackner, W. Koppensteiner, M. Sippl, and F. Domingues. ProSup: a refined tool for protein structure alignment. *Protein Engineering*, 13(11):745 – 752, 2000.
- [24] S. M. Larson, C. D. Snow, M. Shirts, and V. S. Pande. Folding@Home and Genome@Home: Using distributed computing to tackle previously intractable problems in computational biology. *Computational Genomics* (to appear).
- [25] S. Maneewongvatana and D. M. Mount. The analysis of a probabilistic approach to nearest neighbor searching. In *Proc. 7th Workshop on Algorithms and Data Structures (WADS 2001)*, pages 276–286, 2001.
- [26] A. G. Murzin, S. E. Brenner, T. Hubbard, and C. Chothia. SCOP: a structural classification of proteins database for the investigation of sequences and structures. *J. Mol. Biol.*, 247(536-540), 1995.
- [27] S. Needleman and C. Wunsch. A general method applicable to the search for similarities in the amino acid sequence of two proteins. *J. Mol. Biol.*, 48:443 – 453, 1970.
- [28] B. Park and M. Levitt. Energy functions that discriminate X-ray and near-native folds from well-constructed decoys. *J. Mol. Biol.*, 258:367–392, 1996.
- [29] F. P. Preparata and M. I. Shamos. *Computational Geometry: An Introduction*. Springer-Verlag, New York, NY, 1985.
- [30] I. Shindyalov and P. Bourne. protein structure alignment by incremental combinatorial extension (CE) of the optimal path. *Protein engineering*, 11(9):739 – 747, 1998.
- [31] M. R. Shirts and V. S. Pande. Mathematical analysis of coupled parallel simulations. *Physical Review Letters*, 86(22):4983–4987, 2001.
- [32] D. Shortle, K. T. Simons, and D. Baker. Clustering of low-energy conformations near the native structures of small proteins. *Biophysics*, 95:11158–11162, 1998.
- [33] K. T. Simons, R. Bonneau, I. Ruczinski, and D. Baker. Ab initio protein structure prediction of CASP III targets using ROSETTA. *Proteins*, 37(3):171–176, 1999.
- [34] A. P. Singh and D. L. Brutlag. Protein structure alignment: A comparison of methods, 2000. (<http://cmgm.stanford.edu/~brutlag/Abstracts/...singh00.html>).
- [35] G. Song and N. M. Amato. Using motion planning to study protein folding pathways. In *RECOMB*, pages 287–296, 2001.
- [36] E. J. Stollnitz, T. D. DeRose, and D. H. Salesin. Wavelets for computer graphics: A primer (part 1). *IEEE Computer Graphics and Applications*, 15(3):76–84, 1995.
- [37] W. R. Taylor and C. A. Orengo. Protein structure alignment. *J. Mol. Biol.*, 208:1–22, 1989.
- [38] B. Zagrovic, E. J. Sorin, and V. Pande.  $\beta$ -hairpin folding simulations in atomistic detail using an implicit solvent model. *J. Mol. Biol.*, 313:151–169, 2001.